Comparative analysis of CYP2C8-medidated drug-drug interactions produced by CYP2C8 inhibitors, gemfibrozil versus clopidogrel, focusing on the inhibition of drug distribution in UDP-glucuronosyltransferase prior to oxidation

Katsumi Iga (kiga2020@outlook.jp)

Doshisha Women's College of Liberal Arts: Doshisha Joshi Daigaku https://orcid.org/0000-0002-5459-2924

Akiko Kiriyama

Doshisha Women's College of Liberal Arts: Doshisha Joshi Daigaku

Research Article

Keywords: Clopidogrel, CYP2C8, Drug-drug interaction, Gemfibrozil, UDP-glucuronosyltransferase

Posted Date: January 9th, 2023

DOI: https://doi.org/10.21203/rs.3.rs-2364592/v1

Comparative analysis of CYP2C8-mediated drug-drug interactions produced by CYP2C8 inhibitors, gemfibrozil versus clopidogrel, focusing on the inhibition of drug distribution in UDP-glucuronosyltransferase prior to oxidation

KATSUMI IGA[1,2], AKIKO KIRIYAMA[1]

[1] Department of Clinical Pharmacy, Faculty of Pharmaceutical Sciences, Doshisha Women's College of Liberal Arts,
Kodo Kyotanabe-shi, Kyoto 610-0395, Japan

[2] Pre-formulation Department, Pharmaceutical Research and Technology Division, Towa Pharmaceutical Co., Ltd.,
Kyoto Research Park KISTIC#202, 134, Chudoji Minami machi, Shimogyo-ku, Kyoto 600-8813 Japan

***Correspondence to*: Katsumi Iga (telephone: +81-090-3651-6567; Email: kiga2020@outlook.jp)**

Keywords Clopidogrel, CYP2C8, Drug-drug interaction, Gemfibrozil, UDP-glucuronosyltransferase

Abstract

Purpose It is challenging to predict CYP2C8-mediated drug-drug interactions (DDIs) produced by clopidogrel (Clop) and gemfibrozil (Gem) by maintaining the victim's fractional CYP2C8-mediated clearance ($f_{m,CYP2C8}$) constant. The goal is to develop a comprehensive methodology for this.

Method A model where UDP glucuronosyl transferase (UGT) and CYP work in pairs was devised, under the assumption that CYP2C8 substrates bind UGT before oxidation, and that Gem inhibits UGT and CYP2C8 while Clop inhibits CYP2C8 alone. Overall enzymatic inhibitory activity resulting from DDI was expressed as a function of $f_{m,CYP2C8}$, $f_{m,UGT}$ (fractional UGT-mediated clearance), and perpetrator specific inhibitory activities against CYP2C8 and UGT ($pA_{i,CYP2C8}$ and $pA_{i,UGT(d)}$). Reported DDIs where Clop, Gem, or Gem + itraconazole have victimized montelukast, desloratadine, pioglitazone, repaglinide (OATP1B1 substrate) or cerivastatin (OATP1B1 substrate) were chosen for the analysis. Additionally, a method to simulate the victim's plasma metabolite levels in response to the changes in the plasma unchanged drug levels was devised based on the previous method.

Results The changes in the plasma levels of unchanged drug and metabolite produced by the DDIs were simulated successfully. The results confirmed the DDIs were not affected by the hepatic uptake transporter (OATP1B1). The $pA_{i,CYP2C8}$ values for Clop and Gem were estimated to be 7 (85% inhibition) and 15 (93% inhibition). The $pA_{i,UGT(d)}$ values for Clop and Gem were estimated to be 1 (non-inhibition) and 2 (50% inhibition).

Conclusions To predict CYP2C8 mediated DDIs, information on the victim's $f_{m,CYP2C8}$ and $f_{m,UGT}$ as well as the perpetrator's $pA_{i,CYP2C8}$ and $pA_{i,UGT(d)}$ are the most important.

Abbreviations

$A_{i,overall}$	overall enzymatic inhibitory activity
AUC	area under the plasma drug level curve
AUCR	fold increase of AUC in drug-drug interaction
Cer	cerivastatin
Clop	clopidogrel
CYP	cytochrome P450
DDI	drug-drug interaction
Des	desloratadine
Des-3-OH	3-hydroxydesloratadine
Gem	gemfibrozil
f_M	fractional metabolite forming rate

$f_{m,CYP}$	fractional CYP isoform-mediated clearance
$f_{m,UGT}$	fractional UGT isoform mediated clearance
Itr	itraconazole
Mont	montelukast
$pA_{i,CYP}$	perpetrator specific inhibitory activity against CYP isoform
$pA_{i,UGT(d)}$	perpetrator specific inhibitory activity against drug distribution in UGT
Pio	pioglitazone
SM	simulation
Rep	repaglinide
UGT	UDP glucuronosyl transferase

Introduction

There have been tragic deaths from the combination of sorivudine and fluorouracil [1]. This was caused by an abnormal increase in plasma fluorouracil levels caused by inhibition of the metabolism of fluorouracil by sorivudine. Therefore, it is important for pharmaceutical companies to develop drugs with a minimal risk of drug-drug interactions (DDIs) and to provide information about how to avoid unsafe combinations in medical fields. The correspondent author experienced an unusual increase in the plasma ramelteon levels when combined with fluvoxamine in the clinical trial [AUCR (fold increase of the area under the plasma drug level curve in DDI) =130] [2]. This was caused by the inhibition of all the cytochrome P450 isoforms (CYP1A2; CYP2C19; CYP3A4) which mediate the metabolism of ramelteon by fluvoxamine. However, the margin for safety of ramelteon was large, so it did not lead to a serious situation. Such interaction was anticipated to a certain degree. However, it was more than that, and the true cause has not been known for a long time.

Subsequent research by the authors [3-7] revealed that the unusually large DDI was caused by the very low hepatic availability (F_h) of ramelteon, and derived the theory using the tube-based hepatic extraction model, that the magnitude of the interaction (AUCR) is determined by the overall enzymatic inhibitory activity produced by DDI ($A_{i,overall}$) and F_h of the victim drug as:

$$AUCR = [1/F_h - 1]/[\exp\{-Ln(F_h)/A_{i,overall}\} - 1] \quad (1)$$

or $1/A_{i,overall} = [Ln(AUCR) - Ln(AUCR - 1 + 1/F_h)]/ Ln(F_h)$

where F_h is determined by oral clearance (CL_{oral}), extent of absorption (F_a), intestinal availability (F_g), hepatic blood flow rate (Q_h), and blood-plasma ratio (R_b) as:

$$F_h = Q_h \times R_b/(Q_h \times R_b + CL_{oral} \times F_a \times F_g) \quad (2)$$

whereas $A_{i,overall,}$ is determined, in mechanistic terms, by fractional CYP isoform contributions to the victim clearance ($f_{m,CYP}$s) and perpetrator specific inhibitory activities against CYP isoforms ($pA_{i,CYP}$s) as:

$$1/A_{i,overall} = CL_{int}/CL_{int}(+)$$
$$= f_{m,CYP1A2}/pA_{i,CYP1A2} + f_{m,CYP2C19}/pA_{i,CYP2C19} + f_{m,CYP3A4}/pA_{i,CYP3A4} \quad (3)$$

where (+) is the index of coadministration.

Thus, it was shown that any type of CYP-mediated DDI can be predicted by using these equations and the database of the $pA_{i,CYP}$s of the perpetrators.

CYP2C8-mediated DDIs of interest have been reviewed [8]. However, this kind of DDIs is difficult to predict directly by the method described above. Typical examples are DDIs observed in montelukast (Mont: CYP2C8 substrate) and desloratadine (Des: CYP2C8 substrate) when administered with clopidogrel (Clop: CYP2C8 inhibitor) or gemfibrozil (Gem: CYP2C8 inhibitor) [9-11]. It was noted that although the AUCR value for Mont + Gem was larger than for Mont + Clop depending on the in vitro $pA_{i,CYP2C8,}$ the $f_{m,CYP2C8}$ value estimated from a simple relationship with AUCR and $pA_{i,CYP2C8}$ [$f_{m,CYP2C8}$ =(1-1/AUCR)/(1-1/$pA_{i,CYP2C8,in\ vitro}$)] was inconsistent between the two DDIs (around 0.55 for Mont + Clop and around 0.7 for Mont + Gem) [9, 10]. A similar difference was observed in the DDIs for Des [11]. In the case where itraconazole (Itr: CYP3A4 inhibitor) was added as a perpetrator, it was also noted that no meaningful difference was observed in the AUCR between Mont + Gem and Mont + Gem + Itr [9], while a large difference was observed between repaglinide (Rep) + Gem and Rep + Gem + Itr [12]. Mont and Des are oxidized by CYP2C8 to produce M6 [9, 10] and Delor-3-OH [11], respectively. However, it was also noted that no meaningful difference was observed in the plasma M6 levels between Mont + Clop and Mont + Gem [9, 10], while the plasma Des-3-OH levels in Des + Gem were considerably lower than in Des + Clop [11]. It is still not clear why such differences exist. If the victim drug is a OATP1B1 substrate and the CYP2C8 inhibitor can inhibit OATP1B1, the prediction of DDI looks more complicated [13-15]. Therefore, to predict the CYP2C8-mediadted DDIs, all issues described above should be resolved.

The corresponding author has also participated in research on sipoglitazar (anti-diabetic drug; https://www.researchgate.net/publication/327663656). This drug is a CYP2C8 substrate as well. However, it is very unusual in that it binds UDP-glucuronosyl transferase 2B15 (UGT2B15) prior to oxidizing to M1 [16, 17]. In clinical trials, the genetic polymorphism of UGT2B15 was associated with the elimination of the unchanged drug, and the initial plasma M1 levels increased in the group where the unchanged drug was quickly eliminated [18], suggesting a system in which UGT and CYP2C8 work in pairs (UGT-CYP paired system). This phenomenon was quite particular, but a similar phenomenon was also

observed for Des. It was reported that prior to CYP2C8-mediated oxidation, Des binds UGT2B10 and is metabolized by the UGT to Des-N-glu (N-glucuronide) [19]. From this information, it can be inferred that the step at which a CYP2C8 substrate binds to the UGT and forms a glucuronosyl conjugate prior to oxidation is common to all CYP2C8-mediated oxidations [20].

Thus, in the present study, the following model (Figure 1) was devised to predict CYP2C8-mediated DDIs, referring to literature [8, 21-29]. The figure depicts CYP2C8-mediated oxidation using a UGT-CYP paired system, with an example of Mont. When Mont is oxidized by CYP2C8, a fraction of the drug ($f_{m,(UGT\text{-}CYP)}$) first enters through the membrane of the endoplasmic reticulum (ER) into the lumen and is distributed to the inner space of the UGT1A, and part of the drug ($f_{m,UGT(UGT\text{-}CY)}$) is metabolized to M1 (acyl glucuronide) and secreted into the ER lumen, while the remainder ($f_{m,CYP2C8\ (UGT\text{-}CYP)}$) is transferred to the CYP2C8 expressed on the opposite side through the ER membrane to be metabolized to M6 [8, 21-24]. Fig. 1 also shows hypothetically that Clop and Gem act differently to inhibit the metabolism of Mont [10, 25-29], thus resolving the inconsistent $f_{m,CYP2C8}$ issue. That is, Clop inhibits CYP2C8, while Gem inhibits both CYP2C8 and UGT. However, the UGT inhibition by Gem may be characterized by the simple inhibition of the distribution of the drug in the inner space of the UGT ($pA_{i,UGT(d)}$: the letter d stands for distribution), rather than the direct inhibition of UGT-isoform dependent glucuronidation of the drug, because the inhibition appears not specific to the isoform of UGT [24 27]. Moreover, Fig. 1 shows that the small but meaningful contributions of enzymes ($f_{m,CYP3A4}$ and $f_{m,CYP2C9}$ for Mont; $f_{m,CYP3A4}$ for Des) other than that of the two enzymatic pairs ($f_{m,(UGT\text{-}CYP)}$) are also important to determine the plasma metabolite levels [27, 28], and that Clop and Gem exhibit higher inhibition activity against CYP2C8 after glucuronidation [30, 31].

Therefore, the purposes of the study were (i) to analyze the CYP2C8-mediated DDIs produced by Clop and Gem comparatively, based on the UGT-CYP paired model; (ii) to determine the inhibitory activities of these inhibitors against the CYP2C8-mediated oxidation ($pA_{i,CYP2C8}$) and the drug distribution to the UGT ($pA_{i,UGT(d)}$) to predict the DDIs, while resolving the inconsistent $f_{m,CYP2C8}$ issue; (iii) to develop a method for simulating plasma metabolite levels in response to changes in plasma unchanged drug levels, in order to confirm the paired model analysis; finally (iv) to confirm whether this model can predict CYP2C8-mediated drug interactions, independently of hepatic uptake transporters.

Materials and Methods

CYP2C8-mediadted DDIs used for UGT-CYP paired model analysis

CYP2C8-mediated DDIs where Clop, Gem, or Gem + Itr victimized Mont [9, 10], Des [11], pioglitazone (Pio) [32, 33], Rep [12, 34] and cerivastatin (Cer) [35], were chosen for the UGT-CYP paired model analysis.

Plasma level data

The data on the plasma unchanged drug and metabolite levels used in the analysis were read from the graphs in the respective literature.

Calculation of plasma unchanged drug levels

The plasma unchanged drug levels after administration of Mont or Des without or with the perpetrators ($C_{p,oral}$ (t) and $C_{p,oral}$ (+)(t)), were calculated using the static 2-compartment model-based model, as described in the previous report (detailed procedures are found in Supplementary Material 1) [6, 7].

Calculation of $A_{i,overall}$ from F_h and AUCR values

The $A_{i,overall}$ values were calculated from the respective F_h and AUCR values using Eqs. 1 and 2.

Calculation of $f_{m,CYP2C8}$, $f_{m,UGT}$, and $pA_{i,UGT(d)}$ for Mont and Des victimized DDIs in UGT-CYP paired model analysis

The following two equations were applied to the UGT-CYP paired model analysis, assuming Mont is metabolized by CYP3A4, CYP2C9, CYP2C8, and UGT1A [10], while Des is metabolized by CYP3A4, CYP2C8, and UGT2B10 [11].

$$f_{m,CYP3A4}/pA_{i,CYP3A4} + f_{m,CYP2C9} + f_{m,\,(UGT\text{-}CYP)}/A_{i,(UCT\text{-}CYP)} = 1/A_{i,overall} \quad (4)$$

where $f_{m,CYP3A4} + f_{m,CYP2C9} + f_{m,(UGT\text{-}CYP)} = 1$, and $A_{i,(UCT\text{-}CYP)}$ represents total inhibitory activity produced in the UGT-CYP paired system (secondary parameter),

$$f_{m,UGT\ (UGT\text{-}CYP)} + f_{m,CYP2C8\ (UGT\text{-}CYP)}/pA_{i,CYP2C8} = 1/A_{i,CYP2C8\ (UGT\text{-}CYP)} \quad (5)$$

where $f_{m,UGT\ (UGT\text{-}CYP)} + f_{m,CYP2C8\ (UGT\text{-}CYP})$ =1, and $A_{i,CYP2C8\ (UGT\text{-}CYP)}$ represents the inhibitory activity derived from the CYP2C8 inhibition in the UGT-CYP paired system (secondary parameter).

$A_{i,(UCTCYP)}$ and $A_{i,CYP2C8\ (UGT\text{-}CYP)}$ were calculated by inserting appropriate values for $f_{m,CYP3A4}$, $f_{m,CYP2C9}$, $f_{m,CYP2C8\ (UGT\text{-}CYP)}$, $pA_{i,CYP3A4}$ and $pA_{i,CYP2C8}$ into the equations, followed by $pA_{i,UGT(d)}$ [= $A_{i,(UCTCYP)}$/ $A_{i,CYP2C8\ (UGT\text{-}CYP)}$], $f_{m,CYP2C8}$ [= $f_{m,\ (UGT\text{-}CYP)}$ X $f_{m,CYP2C8\ (UGT\text{-}CYP)}$] and $f_{m.UGT}$ [= $f_{m,\ (UGT\text{-}CYP)}$ X $f_{m,UGT\ (UGT\text{-}CYP)}$]. Table 1 provides an overview of the parameters and equations used for the UGT-CYP paired model analysis.

Simulation (SM) of Mont and Des victimized DDIs based on $f_{m,CYP}$s, $f_{m,UGT}$, $pA_{i,CYP2C8}$

and $pA_{i,UGT(d)}$

The five DDIs (Mont + Clop; Mont+ Gem; Mont + Gem + Itr; Des + Clop; Des + Gem), were simultaneously simulated based on $f_{m,CYP}$s, $f_{m,UGT}$, $pA_{i,CYP2C8}$ and $pA_{i,UGT(d)}$, using the UGT-CYP paired model. The SMs were optimized to achieve the lack of UGT inhibition by Clop ($pA_{i,UGT(d)}$ ≈1) and meaningful inhibition by Gem ($pA_{i,UGT(d)}$ >1), by adjusting the input parameters ($f_{m,CYP3A4}$, $f_{m,CYP2C9}$, $f_{m,CYP2C8(UGT-CYP)}$ and $pA_{i,CYP2C8}$), while the $A_{i,overall}$ values were fixed. The initial values of $f_{m,CYP3A4}$ and $f_{m,CYP2C9}$ for Mont were determined with reference to the reported in vitro data [27, 28], while the initial value of $f_{m,CYP3A4}$ for Des was determined with reference to the reported DDI (Des + erythromycin [36]; Des + ketoconazole [37]). The initial $pA_{i,CYP2C8}$ values for Clop and Gem were calculated based on reported in vitro data where Clop-O-glu and Gem-O-glu were assumed to completely determine the inhibitory activities to CYP2C8 [11, 38-40] (detailed calculation can be found in Supplementary Material 2). The final values of $pA_{i,CYP2C8}$ and $pA_{i,UGT(d)}$ were identified as the in vivo values differentiated from those in vitro.

Calculation of plasma metabolite levels in relation to fractional metabolite-forming rate (f_M) for Mont and Des victimized DDIs

Theoretically, the plasma metabolite level at time t [$C_{p,M}$ (t)] is determined by the formation rate of the metabolite in response to the unchanged drug level [$C_{p,}$(t)] as well as the elimination rate of the metabolite ($K_{e,M}$)(Figure 2). If the parent drug is not subject to the hepatic first pass effects, the metabolite is formed during the circulation of the parent drug, and accordingly, the time-dependent rate of the metabolite formation can be shown by the product of f_M and AUC(t)/AUC_∞ of the unchanged drug (Fig. 2b). Meanwhile, if the parent drug is subject to the hepatic first pass effects, the metabolite is formed also during the first pass of the parent drug. Therefore, $C_{p,M}$(t) is expressed as the sum of the plasma level of the metabolite formed during the hepatic first pass of the parent drug [$C_{p,M(1)}$(t)] and the plasma level of the metabolite formed during the systemic circulation of the parent drug [$C_{p,M(2)}$(t)].

The equations for $C_{p,M(1)}$(t) and $C_{p,M(2)}$(t) can be expressed as:

$$C_{p,M(1)}(t) = \int f_M \times D \times (F_a \times F_g - F) \times [dInput(T)/dT] \times F_{h,M\ (eff)} \times G(t-T) dT \quad (6)$$

$$C_{p,M(2)}(t) = \int f_M \times CL_{oral} \times C_p(T) \times G(t-T) dT \quad (7)$$

where $dInput(T)/dT$, $F_{h,M\ (eff)}$ and G(t) represent the absorption rate per unit dose for the unchanged drug, the effective hepatic availability of the metabolite [=1 - $E_{h,M} \times \alpha$: α=0.6], and the function expressing the plasma metabolite level after iv bolus administration of unit dose of the parent drug, respectively.

Thus, the $C_{p,M}$(t) and $C_{p,M}$(+)(t) were calculated using Eq. 6 and Eq. 7 and assuming the same 2-compartment model as $C_{p,}$(t). The detailed procedures can be found in

Supplementary Material 3 (distribution parameters for the metabolite were assumed the same as those of the parent drug).

Results

SMs of plasma unchanged drug levels in Mont and Des victimized DDIs

The plasma unchanged drug levels after administration of Mont or Des without or with Clop, Gem, or Gem + Itr, were successfully simulated (Figure 3). The PK parameters for Mont and Des used for the SMs, can be found in Supplementary Material 4. It was noted that the $F_a \times F_g$ and F_h vales for Mont were 0.6 and 0.97, while those for Des were 1.0 and 0.33, respectively. They were consistent with reported bioavailability values for the respective drugs [41, 42].

$A_{i,overall}$ estimated from F_h and AUCR for Mont and Des victimized DDIs

The $A_{i,overall}$s for the Mont and Des victimized DDIs were shown in Table 2.

It was confirmed that the $A_{i,overall}$s for the Mont DDIs were close to the AUCRs because of the F_h value for Mont is close to unity, while those for the Des DDIs were smaller than the AUCRs because of the F_h value for Des is smaller than unity.

Optimal values of $f_{m,CYP}$s, $pA_{i,CYP2C8}$, and $pA_{i,UGT(d)}$ for Mont and Des victimized DDIs in UGT-CYP paired model analysis

The optimal values for the $f_{m,CYP}$s, $pA_{i,CYP2C8}$, and $pA_{i,UGT(d)}$ for the Mont and Des DDIs obtained in the UGT-CYP paired model analysis were shown in Table 3. The $pA_{i,CYP2C8}$ values for Clop and Gem resulted in 7 (in vitro value = 8.4) and 15 (in vitro value = 23.1), respectively, while the $pA_{i,UGT\ (d)}$ values for Clop and Gem resulted in almost 1 (individual figures: 1.01 and 1.03) and almost 2 (individual figures: 2.20, 1.91 and 2.17), respectively. The $f_{m,CYP3A4}$, $f_{m,CYP2C9}$, $f_{m,CYP2C8}$ and $f_{m,UGT1A}$ values for Mont accounted for 0.02, 0.01, 0.55 and 0.42, respectively, while the $f_{m,CYP3A4}$, $f_{m,CYP2C8}$ and $f_{m,UGT1A}$ values for Des accounted for 0.22, 0.59 and 0.19, respectively. Thus, the results provided a comprehensive solution to the issue of inconsistent $f_{m,CYP2C8}$ value. It was noted that the value of $f_{m,CYP2C9}$ (0.01) for Mont was small but meaningful for the formation of the metabolite (M6), as shown in the sensitivity test.

Values determined for $f_{m\ CYP}(+)$s and $f_{m,UGT}(+)$ for Mont and Des victimized DDIs

The changes in the $f_{m,CYP}$s and $f_{m,UGT}$ values of Mont and Des after the coadministration with the inhibitors [$f_{m,CYP}(+)$s and $f_{m,UGT}(+)$] were shown in Figure 4. In all cases, the coadministration decreased the $f_{m,CYP2C8}$ value, while increased the $f_{m,UGT}$ value. The

coadministration also increased the $f_{m,CYP3A4}$ value of Des, while the $f_{m,CYP3A4}$ of Mont did not change much.

Values determined for f_M and $f_M(+)$ for Mont and Des victimized DDIs

Table 4 shows the f_M and $f_M(+)$ values for M6 and Des-3-OH. To calculate f_M, it was assumed that the metabolites formed by CYP2C8 and CYP2C9 for Mont are restricted to M6 ($f_M = f_{m,CYP2C8} + f_{m,CYP2C9}$) [21, 22], while the metabolites formed by CYP2C8 for Des are restricted to Des-3-OH ($f_M = f_{m,CYP2C8}$) [11]. The f_M values for M6 and Des-3-OH were similar (0.56 and 0.58, respectively), while the $f_M(+)$ values for both the metabolites were decreased depending on the DDIs. The $f_M(+)/f_M$ values for Mont + Clop (0.3), Mont + Gem (0.2) and Mont + Gem + Itr (0.2) were similar, while the $f_M(+)/f_M$ for Des + Gem (0.09) was almost one third that for Des + Clop (0.28). The resulting f_M and $f_M(+)$ values were used for the SMs of the plasma metabolite levels to validate the UGT-CYP paired model analysis.

SM of plasma metabolite levels for Mont and Des victimized DDIs

The plasma M6 and Des-3-OH levels for the Mont and Des victimized DDIs were simulated, by inserting the values for f_M and $f_M(+)$ derived from the UGT-CYP paired model analysis and the appropriate values for K_{eM} and $K_{eM}(+)$ into the equation of $C_{p,M}(t)$. The SMs were successfully performed by adjusting K_{eM} = 5/h and K_{eM} (+)= 1.3/h for Mont + Clop; K_{eM} = 4/h and K_{eM} (+) =0.28/h for Mont + Gem; K_{eM} = 4/h and K_{eM} (+)= 0.14/h for Mont + Gem + Itr; K_{eM} = 0.18/h and K_{eM} (+)= 0.13/h for both Des + Clop and Des + Gem (Figure 5). The reduction in K_{eM} up to 3% for Mont + Gem or Mont + Gem + Itr was correlated with the fact that M6 is metabolized fully by CYP2C8 [9]. Meanwhile, no meaningful reduction in K_{eM} for the Des victimized DDIs was correlated with the fact that Des-3-OH is metabolized independently of CYP2C8 [11].

The Des-3-OH levels at initial stages following administration without the inhibitors were shown high. It was confirmed that these elevated levels were due to the metabolism of Des during the first liver passage (F_h = 0.33)(Supplementary Material 5)

Sensitivity of input parameters used in UGT-CYP paired model analysis for Mont victimized DDIs

For the Mont victimized DDIs, it was examined how $pA_{i,UGT(d)}$ and $f_M(+)/f_M$ values are modified depending on the input parameters ($f_{m,CYP3A4}$, $f_{m,CYP2C9}$, $f_{m,CYP2C8\ (UGT\text{-}CYP)}$ and $pA_{i,CYP2C8)}$) which change from the optimal value (Figure 6). Regardless of the changes in the input parameters, the $pA_{i,UGT(d)}$ value for Clop remained constant around unity and that for Gem ranged from 2 to 2.7. Meanwhile, the $f_M(+)/f_M$ values were changed to reflect the changes in

$f_{m,CYP2C9}$, even if the $f_{m,CYP2C9}$ value is small, indicating that the formation of M6 depends both on CYP2C8 and CYP2C9.

Prediction of DDIs observed for five CYP2C8 substrate drugs

The DDIs observed for the five CYP2C8 substrate drugs (Mont, Des, Pio, Rep and Cer; the latter two are also known as a OATP1B1 substrate) when administered with Clop, Gem, or Gem + Itr, were predicted using Eq. 1 and Eq. 8,

$$f_{m,CYP3A4} + f_{m,CYP2C9} + f_{m,CYP2C19} + (f_{m,CYP2C8}/pA_{i,CYP2C8} + f_{m,UGT})/pA_{i,UGT(d)} = 1/A_{i,overall} \quad (8)$$

where $pA_{i,UGT(d)}$ was assumed to be 1 or 2; $pA_{i,CYP3A4}$, and $pA_{i,CYP2C8}$ were the same as shown in Table 3; for Pio, $F_h = 0.952$, $f_{m,CYP3A4} = 0.12$, $f_{m,CYP2C19} = 0.1$, $f_{m,CYP2C8} = 0.655$, and $f_{m,UGT} = 0.125$; for Rep, $F_h = 0.630$, $f_{m,CYP3A4} = 0.08$, $f_{m,CYP2C8} = 0.828$, and $f_{m,UGT} = 0.092$; for Cer, $F_h = 0.844$, $f_{m,CYP3A4} = 0.10$, $f_{m,CYP2C8} = 0.765$, and $f_{m,UGT} = 0.134$. It was shown that the value of $pA_{i,UGT(d)} = 2$ was successful in predicting the DDIs produced by Gem or Gem + Itr, while the value of $pA_{i,UGT(d)} = 1$ (non UGT inhibition) under-predicted them. Contrarily, it was shown that the value of $pA_{i,UGT(d)} = 1$ successfully predicted the DDIs produced by Clop, while the value of $pA_{i,UGT(d)} = 2$ over-predicted them (Figure 7). The DDI of Pio + Gem + Itr was not included in Fig. 7, as it was suggested to reduce the bioavailability of Pio [33]. However, under the assumption of $F_a = 0.75$, the plasma Pio levels in this DDI were successfully simulated in the same model. The predicted AUCR of the Rep + Gem + Itr DDI appeared to be smaller than the observed one. However, this inconsistency could be attributed to the overestimation of the observed AUC calculated from the limited data (the time last, 7h) [12]. The plasma unchanged drug levels after administration of Pio, Rep and Cer without and with the inhibitors were shown in Supplementary Material 6, confirming that CYP2C8-mediated DDIs produced by Clop and Gem are appropriately described in the UGT-CYP paired model.

Discussion

The comparative analysis of the CYP2C8-mediated DDIs produced by Clop and Gem was performed successfully, based on the UGT-CYP paired model. This resulted in new findings about CYP2C8-mediated DDIs.

First, a CYP2C8 substrate drug distributes and binds to the UGT before it oxidizes with CYP2C8. According to the literature [19], it was shown that before oxidation, Des is distributed to the latent UGT2B10 expressed in the ER and undergoes the glucuronidation by this enzyme in the presence of UGDP. However, it is not limited to Des. The analysis on the DDIs of the five CYP2C8 substrate drugs demonstrated that such a system of oxidation works commonly for other CYP2C8 substrates.

Second, the glucuronidation product or UGT-drug conjugate are not completely transferred to the CYP2C8. Part of the glucuronidation product [$f_{m,UGT}$= $f_{m,UGT\ (UGT\text{-}CYP)}$ X $f_{m,(UGT\text{-}CYP)}$] is liberated from the UGT, secreted into the ER lumen and finally into the systemic circulation as a phase II metabolite. Meanwhile, the remainder including the UGT-drug conjugate [$f_{m,CYP2C8}$ = $f_{m,CYP2C8\ (UGT\text{-}CYP)}$ X $f_{m,(UGT\text{-}CYP)}$] is subject to the oxidation by CYP2C8 and secreted into the systemic circulation as a phase I metabolite. This bi-directional metabolic pathway, characterized by $f_{m,UGT}$ and $f_{m,CYP2C8}$, makes a large contribution to the metabolic clearance of the parent drug, and determines the magnitude of DDI. Previously, it was illustrated, regardless of $f_{m,UGT}$, that the glucuronidation product of Des (Des-N-glucuronide) is completely transferred to the CYP2C8 and subject to the oxidation followed by the de-glucuronidation [8, 11, 19]. However, such an illustration would lead to a misunderstanding of the actual Des-victimized DDIs. Indeed, the glucuronidation product of Des (Des-N-glucuronide) has not been detected in vitro or in vivo [19]. However, it does not mean that $f_{m,UGT}$ is negligible. The glucuronidation products of Mont, Pio, Res and sipoglitazar have been detected in vitro or in vivo, and identified to be M1 [10, 28], M7 (N-glucuronide) [43], RG (M7) (acyl glucuronide) [26, 44], and sipoglitazar-G1 [16,17], respectively. This evidence certainly shows the importance of $f_{m,UGT}$. Although the glucuronidation product of Cer has not been detected in the plasma, the lactone form which is produced after the glucuronidation of the parent drug has been detected [33, 45] to demonstrate the importance of $f_{m,UGT}$. In the literature [46], carriers of UGT1A3*2/*1 associated with increased expression of UGT1A3, showed an increase in the AUC of the plasma M1 levels after administration of Mont by approximately 50%, compared to the non-carriers, while the carriers showed a decrease in the AUC of the plasma unchanged drug levels by approximately 20% and a decrease in the AUC of the plasma M6 levels by approximately 50%. The greater decrease in the M6 levels than the unchanged drug levels demonstrated not only the appropriateness of the present UGT-CYP paired model, but also the importance of $f_{m.UGT}$.

Third, Clop inhibits CYP2C8 alone, while Gem inhibits CYP2C8 and UGT. This finding led to the determination of the in vivo $pA_{i,CYP2C8}$ for Clop and the determination of both the in vivo $pA_{i,CYP2C8}$ and $pA_{i,UGT(d)}$ for Gem, and consequently helped resolve the $f_{m,CYP2C8}$ inconsistency issue. The $pA_{i,CYP2C8}$ value of 7 for Clop which corresponds to an 85% inhibition [(1 – 1/$pA_{i,CYP2C8}$) X 100%], was shown non-modifiable in the sensitivity test conducted for the Mont DDIs. Meanwhile, the $pA_{i,CYP2C8}$ value of 15 for Gem which corresponds to an 93% inhibition of the enzyme, was shown modifiable to a larger value in the sensitivity test for the Mont DDIs. However, an excess value of $pA_{i,CYP2C8}$ underestimated the C_{max} of the Des-3-OH level for the Des + Gem DDI. Thus, the value of 15 was regarded as appropriate. The in vitro $pA_{i,CYP2C8}$ values for Clop and Gem were calculated for the preliminary SMs. However,

they were found to be close to the final values in vivo, so that the in vivo values are justified by the in vitro data (Supplementary Material 2).

The $pA_{i,UGT(d)}$ values for Gem determined from the Mont and Des victimized DDIs were approximately 2 (50% inhibition), regardless of the UGT isoforms (Mont: UGT1A3 [28]; DesUGT2B10 [19]). This value of 2 was also found to be applicable for the prediction of the Pio, Rep (substrate of UGT1A3 [26]) and Cer victimized DDIs. Thus, the inhibition of UGT by Gem is regarded as not dependent of the isoform of UGT [26, 29], suggesting the simple inhibition of the drug's distribution to the UGT. In vitro inhibition of glucuronidation of Mont to M1 by Gem has been reported, showing an IC_{50} of 83 μM [28]. Indeed, the IC_{50} value shows no meaningful inhibition effect on the glucuronidation of Mont. However, if the concentration of Gem (or Gem-O-glu) at the UGT is equivalent to the IC_{50}, which is almost three times the maximum plasma level of Gem, then the in vitro $pA_{i,UGT(d)}$ would be similar to the in vivo $pA_{i,UGT(d)}$, so that the in vivo $pA_{i,UGT(d)}$ would be justified by the in vitro data. Ketoconazole was reported to have a strong inhibition to various isoforms of UGT (IC_{50} = 12 μM), the same as Gem in relation to the non-isoform dependency [47-49]. However, it should be noted that the inhibition of Des-3-OH formation by ketoconazole was not large both in vitro [19] and in vivo [37], probably because Ketoconazole does not inhibit CYP2C8. The same would apply to Gem, if Gem does not inhibit CYP2C8: the $A_{i,overall}$ value for Des + Gem ($pA_{i,UGT(d)}$ = 2; $pA_{i,CYP2C8}$ =1) would be calculated to be merely 1.14 (AUCR = 1.2).

The present model analysis provided a better understanding of the changes in AUCR when Itr was added to Mont + Gem or Rep + Gem [4.02 (Mont + Gem + Itr) versus 4.28 (Mont + Gem); 13.9 (Rep + Gem + Itr) versus 7.99 (Rep + Gem)]. That is, the negligible change in AUCR for Mont in contrast to Rep, is attributed not only to the small $f_{m,CYP3A4}$ but also to the large $f_{m,UGT}$. Based on the present model analysis, the extremely small but non-zero value of $f_{m,CYP3A4}$ (0.02) was estimated for Mont. However, the $f_M(+)/f_M$ value for M5 formed by the CYP3A4-mediated oxidation corresponds to $A_{i,overall}$ = 4.2 [AUCR(M5) (obs) = 5.4] for Mont + Gem, and $A_{i,overall}/pA_{i,CYP3A4}$ = 0.8 [AUCR(M5) (obs) = 1.0] for Mont + Gem + Itr, indicating the dependency of the $pA_{i,CYP3A4}$ of Itr, regardless of $f_{m,CYP3A4}$.

The present model analysis also provided a better understanding of the change in the plasma metabolite levels in response to Clop and Gem. Despite the difference in the $pA_{i,CYP2C8}$ value between Clop and Gem, the formation rate [$f_M(+)$] of M6 from Mont was not much different between Clop and Gem, in contrast to that of Des-3-OH from Des. Indeed, M6 is primarily formed by CYP2C8-mediated oxidation with a small contribution of CYP2C9. However, the present analysis demonstrated even the smallest value of $f_{m,CYP2C9}$ affects the value of $f_M(+)/f_M$ in such a way as to reduce the CYP2C8 inhibitory effect of Clop and Gem [$f_M(+)/f_M = (A_{i,overall} \times f_{m,CYP2C9} + f_{m,CYP2C8}(+))/(f_{m,CYP2C9} + f_{m,CYP2C8})$].

The present model analysis of the DDIs of the two OATP1B1 substrates (Rep and Cer) has successfully demonstrated that Gem does not inhibit the hepatic uptake of these drugs by OATP1B1 in vivo. However, contrary to the present finding, model analyses have been reported, emphasizing the increase in AUCR in response to the decrease in hepatic uptake ratio $R_{up}(+)/R_{up}$ when Rep or Cer were administered with Gem [50-53]. The models were all based on physiologically based pharmacokinetic (dynamic) modeling and permeation-limited hepatic disposition model [50]. Unfortunately, they did not provide a clear indication of the extent to which the hepatic uptake inhibition contributed to the DDIs. Indeed, these dynamic model approaches appear difficult to follow in an exact way, but it may be possible on the static basis by using an equation for $R_{up}/R_{up}(+)$ derived from the permeation-limited hepatic disposition model [50] (Supplementary Material 7): $R_{up}/R_{up}(+) = A_{i,overall\ (total)} \times (1 + r)/(A_{i,overall\ (met)} + r)$, where r represents the ratio of the metabolic clearance ($CL_{int,met}$) to the passive permeation clearance (CL_{pd}) (r = 0: hepatic disposition not limited by permeation as in the present study), and $A_{i,overall\ (total)}$ can be calculated from F_h and AUCR using Eq. 1, and $A_{i,overall\ (met)}$ can be calculated from $f_{m,CYP}$s, $f_{m,UGT}$, $pA_{i,CYP}$s, and $pA_{i,UGT(d)}$ using Eq. 8. Our preliminary calculation of $R_{up}/R_{up}(+)$ for Rep + Gem and Rep + Gem + Itr, using the data in the literature [52] [$r = 1/(1/\beta - 1) = 0.48$ ($\beta = 0.324$), $f_{m,CYP2C8} = 0.84$ and $f_{m,CYP3A4} = 0.16$] gave a meaningful value of 1.89 and 1.39 for each. However, $R_{up}/R_{up}(+)$ for Rep + Clop also resulted in a meaningful value of 1.26, contrary to the common belief that Clop does not inhibit OATP1B1. This calculation did not account for $f_{m,UGT}$. However, when we recalculated assuming the same values of $f_{m,CYP}$s and $f_{m,UGT}$ as obtained in the present study, the $R_{up}/R_{up}(+)$ for Rep + Clop, Rep + Gem and Rep + Gem + Itr resulted in 1.30, 1.33 and 1.34, respectively, suggesting that both Gem and Clop inhibit OATP1B1 in the same way, opposing to their expectation. It should be noted that the value of r is variable based on a modifiable empirical scaling factor used to bind in vitro to in vivo [50, 54, 55]. As such, there may be uncertainty with r [54]. Indeed, the literature [50] has proposed a 5-7 times larger value of 2.47 than 0.36 [51], 0.48 [52] and 0.49 [54]. However, it gives a $R_{up}/R_{up}(+)$ larger than unity (2.02) for Rep + Clop, making it more difficult to explain. Thus, these calculations confirm not only that Gem does not inhibit hepatic uptake transporter OATP1B1 in vivo, but that the hepatic disposition of Rep and Cer including other CYP2C8 substrates is not limited by the hepatic permeability.

The method of simulating plasma metabolite level was originally developed in this study. In combination with the present UGT-CYP paired model, it has proven useful for the analysis of CYP2C8-mediated DDIs. Primarily, the method employs two kinds of metabolite specific parameters (f_M and K_{eM}), along with the PK parameters of the unchanged drug. Developing the method has led to new findings. The plasma metabolite level is affected by the hepatic first pass effect of the unchanged drug. It is also affected by the hepatic first pass effect of

the metabolite itself. That is, the metabolite formed during the first pass of the unchanged drug is subject to the first pass effects on the way to the entrance of the systemic circulation [$F_{h,M\ (eff)}$]. The distribution parameters for the metabolite can be assumed the same as those for the unchanged drug if the metabolite is formed by the oxidation. Therefore, the method allows us to estimate how much the f_M and K_{eM} values will be affected by the DDIs in a simple way, although this has not been possible in the past.

Conclusions

Based on the UGT-CYP paired model, the CYP2C8-mediated DDIs produced by Clop and Gem were successfully predicted, thereby solving the inconsistent $f_{m,CYP2C8}$ issue. The results also confirmed that the DDIs were not affected by the hepatic uptake transporter (OATP1B1). The $pA_{i,CYP2C8}$ values for Clop and Gem were estimated to be 7 (85% inhibition) and 15 (93% inhibition), while the $pA_{i,UGT(d)}$ values for Clop and Gem were estimated to be 1 (non-inhibition) and 2 (50% inhibition). To predict CYP2C8 mediated DDIs, this information proved the most important.

Conflict of Interest

The authors declare no conflict of interest.

Data Availability Statement

All data generated or analyzed during this study are included in this published article and its supplementary information file.

Electronic Supplementary Material

The online version of this article contains supplementary material, which is available to authorized users.

Figure Legends

Figure 1 Illustration of a UGT-CYP paired model to analyze CYP2C8-mediated DDIs produced by Gem and Clop, with an example of Mont. The distribution of Mont into the UGT (UGT1A) from inside the endoplasmic reticulum (ER) occurs first, and then part of the drug

is metabolized to M1 (acyl glucuronide) by this latent enzyme and secreted into the ER lumen as a phase II metabolite, while the remainder is transferred to the CYP2C8 that is adjacent to the UGT and thereby oxidized to a phase I metabolite. In this bi-directional metabolic pathway, Gem inhibits both UGT and CYP2C8 while Clop inhibits CYP2C8 alone. These inhibitors show increased inhibition activity against CYP2C8 after glucuronidation.

Figure 2 Illustration of how to determine the plasma metabolite levels in response to the unchanged drug levels when the first pass effect of a drug is not considered.

Figure 3 Static 2-compartment model-based simulations (SMs) of the plasma unchanged victim levels in the DDIs where Clop, Gem, or Gem + Itr victimized Mont and Des. The doses of Mont, Des, Clop, Gem and Itr were 10mg SD, 5 mg SD, 300mg then 75mg QD X 3 days, 600 mg BID X 3 days, and 100mg QD X 3 days, respectively. (-): control; (+): coadministration; obs: observed.

Figure 4 Changes in the fractional enzymatic clearances ($f_{m,CYP}$s and $f_{m,UGT}$) determined for the Mont and Des victimized DDIs.

$f_{m,CYP3A4}(+) = A_{i,overall} \times f_{m,CYP3A4}/pA_{i,CYP3A4}$

$f_{m,CYP2C9}(+) = A_{i,overall} \times f_{m,CYP2C9}$

$f_{m,CYP2C8}(+) = A_{i,overall} \times f_{m,CYP2C8}/pA_{i,UGT(d)}/pA_{i,CYP2C8}$

$f_{m,UGT}(+) = A_{i,overall} \times f_{m,UGT}/pA_{i,UGT(d)}$

Figure 5 f_M-based SMs of the plasma levels of metabolites formed by CYP2C8, in response to the unchanged drug levels in the DDIs where Clop, Gem, or Gem + Itr victimized Mont and Des.

Figure 6 Sensitivity of the input parameters used in the UGT-CYP paired model analysis to $f_M(+)/f_M$ and $pA_{i,UGT(d)}$ for Mont victimized DDIs (optimal parameters are centered).

Figure 7 Prediction of AUCR for the DDIs in which Clop, Gem, or Gem + Itr victimized Mont, Des, Pio, Rep, and Cer, assuming inhibition of UGT ($pA_{i,UGT(d)} = 2$), compared with the noninhibition ($pA_{i,UGT(d)} = 1$). For Pio, $F_h = 0.952$, $f_{mCYP3A4} = 0.12$, $f_{m,CYP2C19} = 0.1$, $f_{m,CYP2C8} = 0.655$ and $f_{m,UGT} = 0.125$ were assumed. For Rep, $F_h = 0.630$, $f_{mCYP3A4} = 0.08$, $f_{m,CYP2C8} = 0.828$ and $f_{m,UGT} = 0.092$ were assumed. For Cer, $F_h = 0.844$, $f_{mCYP3A4} = 0.10$, $f_{m,CYP2C8} = 0.765$ and $f_{m,UGT} = 0.135$ were assumed. The observed AUCR for Rep + Gem + Itr (*) would not necessarily be accurate because the time last (7h) was too short to estimate the AUC $(+)_\infty$.

Table 1 Overview of parameters and equations used for the UGT-CYP paired model analysis.

Parameters	Equations for determination
$A_{i,overall}$ (input)	Eq. 1
$pA_{i,CYP3A4}$ (input)	$1 + I_u/K_{iu,CYP3A4}$
$pA_{i,CYP2C8}$ (input)	$1 + I_u/K_{iu,CYP2C8}$
$f_{m,CYP3A4}$ (input)	
$f_{m,CYP2C9}$ (input)	
Secondary parameters	
$f_{m,(UGT\text{-}CYP)}$ [a] (output)	$1 - f_{m,CYP3A4} - f_{m,CYP2C9}$
$A_{i,(UGT\text{-}CYP)}$ [b] (output)	Eq. 4
$f_{m,\ CYP2C8\ (UGT\text{-}CYP)}$ [c] (input)	
$f_{m,\ UGT\ (UGT\text{-}CYP)}$ [d] (output)	$1 - f_{m,CYP2C8\ (UGT\text{-}CYP)}$
$A_{i,CYP2C8\ (UGT\text{-}CYP)}$ [e] (output)	Eq. 5
$f_{m,CYP2C8}$ (output)	$f_{m,(UGT\text{-}CYP)} \times f_{m,CYP2C8\ (UGT\text{-}CYP)}$
$f_{m,UGT}$ (output)	$f_{m,(UGT\text{-}CYP)} \times f_{m,UGT\ (UGT\text{-}CYP)}$
$pA_{i,UGT\ (d)}$ (output)	$A_{i,(UGT\text{-}CYP)}/A_{i,CYP2C8\ (UGT\text{-}CYP)}$

a) fractional metabolic clearance mediated by the UGT-CYP enzyme pair to the total clearance.

b) total inhibitory activity produced in the UGT-CYP enzyme pair system.

c) fractional clearance mediated by CYP2C8 in the UGT-CYP enzyme pair system.

d) fractional clearance mediated by UGT in the UGT-CYP enzyme pair system.

e) inhibitory activity derived from CYP2C8 inhibition in the UGT-CYP pair system.

Table 2 $A_{i,overall}$s determined for the DDIs in which Mont and Des were victimized.

	Input/output	Mont + Clop	Mont + Gem	Mont + Gem + Itr	Des + Clop	Des + Gem
AUCR	Input	1.98	4.28	4.02	2.80	4.62
CL_{oral} (L/h)	Input	3.13	3.18	3.18	109	109
F_h	Output	0.966	0.966	0.966	0.332	0.332
$A_{i,overall}$	Output	1.96	4.22	3.97	2.04	3.05

Table 3 Input-and-output parameters determined using the UGT-CYP paired model to correspond to the DDIs in which Mont and Des were victimized.

	Input/output	Mont + Clop	Mont + Gem	Mont + Gem + Itr	Des + Clop	Des + Gem
$pA_{i,CYP3A4}$ [a)]	Input	1	1	5	1	1
$pA_{i,CYP2C8}$	Input	7	15	15	7	15
$f_{m,CYP3A4}$	Input	0.02	0.02	0.02	0.22	0.22
$f_{m,CYP2C9}$	Input	0.01	0.01	0.01	0	0
$f_{m,(UGT-CYP)}$	Output	0.97	0.97	0.97	0.78	0.78
$A_{i,(UGT-CYP)}$	Output	2.02	4.69	4.08	2.88	7.23
$f_{m,\ CYP2C8\ (UGT-CYP)}$	Input	0.57	0.57	0.57	0.75	0.75
$f_{m,\ UGT\ (UGT-CYP)}$	Output	0.43	0.43	0.43	0.25	0.25
$A_{i,CYP2C8\ (UGT-CYP)}$	Output	1.96	2.14	2.14	2.80	3.33
$f_{m,CYP2C8}$	Output	0.55	0.55	0.55	0.59	0.59
$f_{m,UGT}$	Output	0.42	0.42	0.42	0.19	0.19
$pA_{i,UGT\ (d)}$	Output	1.03	2.20	1.91	1.03	2.17

[a)] $pA_{i,CYP3A4}$ for Itr was assumed to be half the previous reported one (Ref 6), considering of interaction with Gem.

Table 4 The values of f_M and $f_M(+)$ for M6 and Des-3-OH.

	Calculation	Mont + Clop	Mont + Gem	Mont + Gem + Itr	Des + Clop	Des + Gem
f_M	$f_{m,CYP2C9} + f_{m,CYP2C8}$	0.563	0.563	0.563	0.585	0.585
$f_M(+)$	$f_{m,CYP2C9}(+) + f_{m,CYP2C8}(+)$	0.169	0.113	0.116	0.166	0.055
$f_M(+)/f_M$		0.301	0.201	0.207	0.283	0.094

References

1. Okuda H, Nishiyama T, Ogura K, Nagayama S, Ikeda K, Yamaguchi S, Nakamura Y, Kawaguchi Y, Watabe T. Lethal drug interactions of sorivudine, a new antiviral drug, with oral 5-fluorouracil prodrugs. Drug Metab Dispos. 1997; 25 (5): 270-3.

2. Sateia MJ, Kirby-Long P, Taylor JL. Efficacy and clinical safety of ramelteon: an evidence-based review. Sleep Med Rev. 2008; 12 (4): 319-32.

3. Iga K. Use of three-compartment physiologically based pharmacokinetic modeling to predict hepatic blood levels of fluvoxamine relevant for drug-drug interactions. J Pharm Sci. 2015; 104 (4): 1478-91.

4. Iga K. Simulation of metabolic drug-drug interactions perpetrated by fluvoxamine using hybridized two-compartment hepatic drug-pool-based tube modeling and estimation of in vivo inhibition constants. J Pharm Sci. 2015; 104 (10): 3565-77.

5. Iga K. Dynamic and static simulations of fluvoxamine-perpetrated drug-drug interactions using multiple cytochrome P450 inhibition modeling, and determination of perpetrator-specific CYP isoform inhibition constants and fractional CYP isoform contributions to victim clearance. J Pharm Sci. 2016; 105 (3): 1307-17.

6. Iga K, Kiriyama A. Simulations of cytochrome P450 3A4-mediated drug-drug interactions by simple two-compartment model-assisted static method. J Pharm Sci. 2017; 106 (5): 1426-1438.

7. Iga K, Kiriyama A. Usefulness of two-compartment model-assisted and static overall inhibitory-activity method for prediction of drug-drug interaction. Biol Pharm Bull. 2017; 40 (12): 2024-37.

8. Backman JT, Filppula AM, Niemi M, Neuvonen PJ. Role of cytochrome P450 2C8 in drug metabolism and interactions. Pharmacol Rev. 2016; 68 (1): 168-241.

9. Karonen T, Neuvonen PJ, Backman JT. CYP2C8 but not CYP3A4 is important in the pharmacokinetics of montelukast. Br J Clin Pharmacol. 2012; 73 (2): 257-67.

10. Itkonen MK, Tornio A, Filppula AM, Neuvonen M, Neuvonen PJ, Niemi M, Backman JT. Clopidogrel but not prasugrel significantly inhibits the CYP2C8-mediated metabolism of montelukast in humans. Clin Pharmacol Ther. 2018; 104 (3): 495-504.

11. Itkonen MK, Tornio A, Neuvonen M, Neuvonen PJ, Niemi M, Backman JT. Clopidogrel and gemfibrozil strongly inhibit the CYP2C8-dependent formation of 3-hydroxydesloratadine and increase desloratadine exposure in humans. Drug Metab Dispos. 2019; 47 (4): 377-85.

12. Niemi M, Backman JT, Neuvonen M, Neuvonen PJ. Effects of gemfibrozil, itraconazole, and their combination on the pharmacokinetics and pharmacodynamics of repaglinide: potentially hazardous interaction between gemfibrozil and repaglinide. Diabetologia. 2003; 46 (3): 347-51.

13. Shitara Y, Itoh T, Sato H, Li AP, Sugiyama Y. Inhibition of transporter-mediated hepatic uptake as a mechanism for drug-drug interaction between cerivastatin and cyclosporin A. J Pharmacol Exp Ther. 2003; 304 (2): 610-6.

14. Yoshida K, Maeda K, Sugiyama Y, Transporter-mediated drug--drug interactions involving OATP substrates: predictions based on in vitro inhibition studies. Clin Pharmacol Ther. 2012; 91 (6): 1053-64

15. Tornio A, Neuvonen PJ, Niemi M, Backman JT. Role of gemfibrozil as an inhibitor of CYP2C8 and membrane transporters. Expert Opin Drug Metab Toxicol. 2017; 13 (1): 83-95.

16. Nishihara M, Sudo M, Kamiguchi H, Kawaguchi N, Maeshiba Y, Kiyota Y, Takahashi J, Tagawa Y, Kondo T, Asahi S. Metabolic fate of sipoglitazar, a novel oral PPAR agonist with activities for PPAR-γ, -α and -δ, in rats and monkeys and comparison with humans in vitro. Drug Metab Pharmacokinet. 2012; 27 (2): 223-31.

17. Nishihara M, Sudo M, Kawaguchi N, Takahashi J, Kiyota Y, Kondo T, Asahi S. An unusual metabolic pathway of sipoglitazar, a novel antidiabetic agent: cytochrome P450-catalyzed oxidation of sipoglitazar acyl glucuronide. Drug Metab Dispos. 2012; 40 (2): 249-58.

18. Stringer F, Scott G, Valbuena M, Kinley J, Nishihara M, Urquhart R. The effect of genetic polymorphisms in UGT2B15 on the pharmacokinetic profile of sipoglitazar, a novel anti-diabetic agent. Eur J Clin Pharmacol. 2013; 69 (3): 423-30.

19. Kazmi F, Barbara JE, Yerino P, Parkinson A. A long-standing mystery solved: the formation of 3-hydroxydesloratadine is catalyzed by CYP2C8 but prior glucuronidation of desloratadine by UDP-glucuronosyltransferase 2B10 is an obligatory requirement. Drug Metab Dispos. 2015; 43 (4): 523-33.

20. Ma Y, Fu Y, Khojasteh SC, Dalvie D, Zhang D. Glucuronides as potential anionic substrates of human cytochrome P450 2C8 (CYP2C8). J Med Chem. 2017; 60 (21): 8691-705.

21. Fujiwara R, Yokoi T, Nakajima M. Structure and protein-protein interactions of human UDP-glucuronosyltransferases. Front Pharmacol. 2016; 7: 388.

22. Liu Y, Coughtrie MWH. Revisiting the latency of uridine diphosphate-glucuronosyltransferases (UGTs)-how does the endoplasmic reticulum membrane influence their function? Pharmaceutics. 2017; 9 (3): 32.

23. Hu G, Johnson EF, Kemper B. CYP2C8 exists as a dimer in natural membranes. Drug Metab Dispos. 2010; 38 (11): 1976-83.

24. Kazmi F, Yerino P, Barbara JE Parkinson A. Further characterization of the metabolism of desloratadine and its cytochrome P450 and UDP-glucuronosyltransferase inhibition potential: identification of desloratadine as a relatively selective UGT2B10 inhibitor. Drug Metab Dispos. 2015, 43: 1294-302.

25. Parkinson A, Kazmi F, Buckley DB, Yerino P, Ogilvie BW, Paris BL. System-dependent outcomes during the evaluation of drug candidates as inhibitors of cytochrome P450 (CYP) and uridine diphosphate glucuronosyltransferase (UGT) enzymes: human hepatocytes versus liver microsomes versus recombinant enzymes. Drug Metab Pharmacokinet. 2010; 25 (1): 16-27.

26. Gan J, Chen W, Shen H, Gao L, Hong Y, Tian Y, Li W, Zhang Y, Tang Y, Zhang H, Humphreys WG, Rodrigues AD. Repaglinide-gemfibrozil drug interaction: inhibition of repaglinide glucuronidation as a potential additional contributing mechanism. Br J Clin Pharmacol. 2010; 70 (6): 870-80.

27. VandenbBrink BM, Foti RS, Rock DA, Wienkers LC, Wahlstrom JL. Evaluation of CYP2C8 inhibition in vitro: utility of montelukast as a selective CYP2C8 probe substrate. Drug Metab Dispos. 2011; 39 (9):1546-54.

28. Cardoso JO, Oliveira RV, Lu JBL, Desta Z. In vitro metabolism of montelukast by cytochrome P450s and UDP-glucuronosyltransferases. Drug Metab Dispos. 2015; 43 (12): 1905-16.

29. Kahma H, Filppula AM, Neuvonen M, Tarkiainen EK, Tornio A, Holmberg MT, Itkonen MK, Finel M, Neuvonen PJ, Niemi M, Backman JT. Clopidogrel carboxylic acid glucuronidation is mediated mainly by UGT2B7, UGT2B4, and UGT2B17: implications for pharmacogenetics and drug-drug interactions. Drug Metab Dispos. 2018; 46 (2): 141-150.

30. Shitara Y, Hirano M, Sato H, Sugiyama Y. Gemfibrozil and its glucuronide inhibit the organic anion transporting polypeptide 2 (OATP2/OATP1B1:SLC21A6)-mediated hepatic uptake and CYP2C8-mediated metabolism of cerivastatin: analysis of the mechanism of the clinically relevant drug-drug interaction between cerivastatin and gemfibrozil. J Pharmacol Exp Ther. 2004; 311 (1): 228-36.

31. Shah MB. Inhibition of CYP2C8 by acyl glucuronides of gemfibrozil and clopidogrel: pharmacological significance, progress and challenges. Biomolecules. 2022; 12 (9): 1218.

32. Jaakkola T, Backman JT, Neuvonen M, Neuvonen PJ. Effects of gemfibrozil, itraconazole, and their combination on the pharmacokinetics of pioglitazone. Clin Pharmacol Ther. 2005; 77 (5): 404-14.

33. Itkonen MK, Tornio A, Neuvonen M, Neuvonen PJ, Niemi M, Backman JT. Clopidogrel markedly increases plasma concentrations of CYP2C8 substrate pioglitazone. Drug Metab Dispos. 2016; 44 (8): 1364-71.

34. Tornio A, Filppula AM, Kailari O, Neuvonen M, Nyrönen TH, T Tapaninen T, Neuvonen PJ, Niemi M, Backman JT. Glucuronidation converts clopidogrel to a strong time-dependent inhibitor of CYP2C8: a phase II metabolite as a perpetrator of drug-drug interactions. Clin Pharmacol Ther. 2014; 96 (4) :4 98-507.

35. Backman JT, Kyrklund C, Neuvonen M, Neuvonen PJ. Gemfibrozil greatly increases plasma concentrations of cerivastatin. Clin Pharmacol Ther. 2002; 72 (6): 685-91.

36. Banfield C, Hunt T, Reyderman L, Statkevich P, Padhi D, Affrime M. Lack of clinically relevant interaction between desloratadine and erythromycin. Clin Pharmacokinet. 2002; 41 Suppl 1: 29-35.

37. Banfield C, Herron J, Keung A, Padhi D, Affrime M. Desloratadine has no clinically relevant electrocardiographic or pharmacodynamic interactions with ketoconazole. Clin Pharmacokinet. 2002; 41 Suppl 1: 37-44.

38. Ogilvie BW, Zhang D, Li W, Rodrigues AD, Gipson AE, Holsapple J, Toren P, Parkinson A. Glucuronidation converts gemfibrozil to a potent, metabolism-dependent inhibitor of CYP2C8: implications for drug-drug interactions. Drug Metab Dispos. 2006; 34 (1):191-7.

39. Backman JT, Honkalammi J, Neuvonen M, Kurkinen KJ, Tornio A, Niemi M, Neuvonen PJ. CYP2C8 activity recovers within 96 hours after gemfibrozil dosing: estimation of CYP2C8 half-life using repaglinide as an in vivo probe. Drug Metab Dispos. 2009; 37 (12): 2359-66.

40 Takagi M, Sakamoto M, Itoh T, Fujiwara R. Underlying mechanism of drug-drug interaction between pioglitazone and gemfibrozil: gemfibrozil acyl-glucuronide is a mechanism-based inhibitor of CYP2C8. Drug Metab Pharmacokinet. 2015; 30 (4): 288-94.

41. Cheng H, Leff JA, Amin R, Gertz BJ, Smet MD, Noonan N, Rogers JD, Malbecq W, Meisner D, Somers G. Pharmacokinetics, bioavailability, and safety of montelukast sodium (MK-0476) in healthy males and females. Pharm Res. 1996; 13 (3):445-8.

42. Molimard M, Diquet B, Benedetti MS. Comparison of pharmacokinetics and metabolism of desloratadine, fexofenadine, levocetirizine and mizolastine in humans. Fundam Clin Pharmacol. 2004; 18(4): 399-411.

43. Uchiyama M, Fischer T, Mueller J, Oguchi M, Yamamura N, Koda H, Iwabuchi H, Izumi T. Identification of novel metabolic pathways of pioglitazone in hepatocytes: N-glucuronidation of thiazolidinedione ring and sequential ring-opening pathway. Drug Metab Dispos. 2010; 38 (6): 946-56.

44. Säll C, Houston JB, Galetin A. A comprehensive assessment of repaglinide metabolic pathways: impact of choice of in vitro system and relative enzyme contribution to in vitro clearance. Drug Metab Dispos. 2012; 40 (7):1279-89.

45. Schirris TJJ, Ritschel T, Bilos A, Smeitink JAM, Russel FGM. Statin lactonization by uridine 5'-diphospho-glucuronosyltransferases (UGTs). Mol Pharm. 2015; 12 (11): 4048-55.

46. Hirvensalo P, Tornio A, Neuvonen M, Tapaninen T, Paile-Hyvärinen M, Kärjä V, Männistö VT, Pihlajamäki J, Backman JT, Niemi M. Comprehensive pharmacogenomic study reveals an important role of UGT1A3 in montelukast pharmacokinetics. Clin Pharmacol Ther. 2018; 104 (1):158-168.

47. Bourcier K, Hyland R, Kempshall S, Jones R, Maximilien J, Irvine N, Jones B. Investigation into UDP-glucuronosyltransferase (UGT) enzyme kinetics of imidazole- and triazole-containing antifungal drugs in human liver microsomes and recombinant UGT enzymes. Drug Metab Dispos. 2010; 38 (6): 923-9.

48. Gradinaru J, Romand S, Geiser L, Carrupt PA, Spaggiari D, Rudaz S. Inhibition screening method of microsomal UGTs using the cocktail approach. Eur J Pharm Sci. 2015; 71: 35-45.

49. Pattanawongsa A, Nair PC, Andrew Rowland A, Miners JO. Human UDP-Glucuronosyltransferase (UGT) 2B10: validation of cotinine as a selective probe substrate, inhibition by UGT enzyme-selective inhibitors and antidepressant and antipsychotic drugs, and structural determinants of enzyme inhibition. Drug Metab Dispos. 2016; 44 (3): 378-88.

50. Varma MVS, Lai Y, Kimoto E, Goosen TC, El-Kattan AF, Kumar V. Mechanistic modeling to predict the transporter- and enzyme-mediated drug-drug interactions of repaglinide. Pharm Res. 2013; 30 (4):1188-99.

51. Kudo T, Hisaka A, Sugiyama Y, Ito K. Analysis of the repaglinide concentration increase produced by gemfibrozil and itraconazole based on the inhibition of the hepatic uptake transporter and metabolic enzymes. Drug Metab Dispos. 2013; 41 (2): 362-71.

52. Kim SJ, Toshimoto K, Yao Y, Yoshikado T, Sugiyama Y. Quantitative analysis of complex drug-drug interactions between repaglinide and cyclosporin A/gemfibrozil using

physiologically based pharmacokinetic models with in vitro transporter/enzyme inhibition data. J Pharm Sci. 2017; 106 (9): 2715-2726.

53. Yao Y, Toshimoto K, Kim SJ, Yoshikado T, Sugiyama Y. Quantitative analysis of complex drug-drug interactions between cerivastatin and metabolism/transport inhibitors using physiologically based pharmacokinetic modeling. Drug Metab Dispos. 2018; 46 (7): 924-933.

54. Gertz M, Tsamandouras N, Säll C, Houston JB, Galetin A. Reduced physiologically-based pharmacokinetic model of repaglinide: impact of OATP1B1 and CYP2C8 genotype and source of in vitro data on the prediction of drug-drug interaction risk. Pharm Res. 2014; 31 (9): 2367-82.

55. Varma MV, Kimoto E, Scialis R, Bi Y, Lin J, Eng H, Kalgutkar AS, El-Kattan AF, Rodrigues AD, Tremaine LM. Transporter-mediated hepatic uptake plays an important role in the pharmacokinetics and drug-drug interactions of montelukast. Clin Pharmacol Ther. 2017; 101 (3): 406-415.

Figures

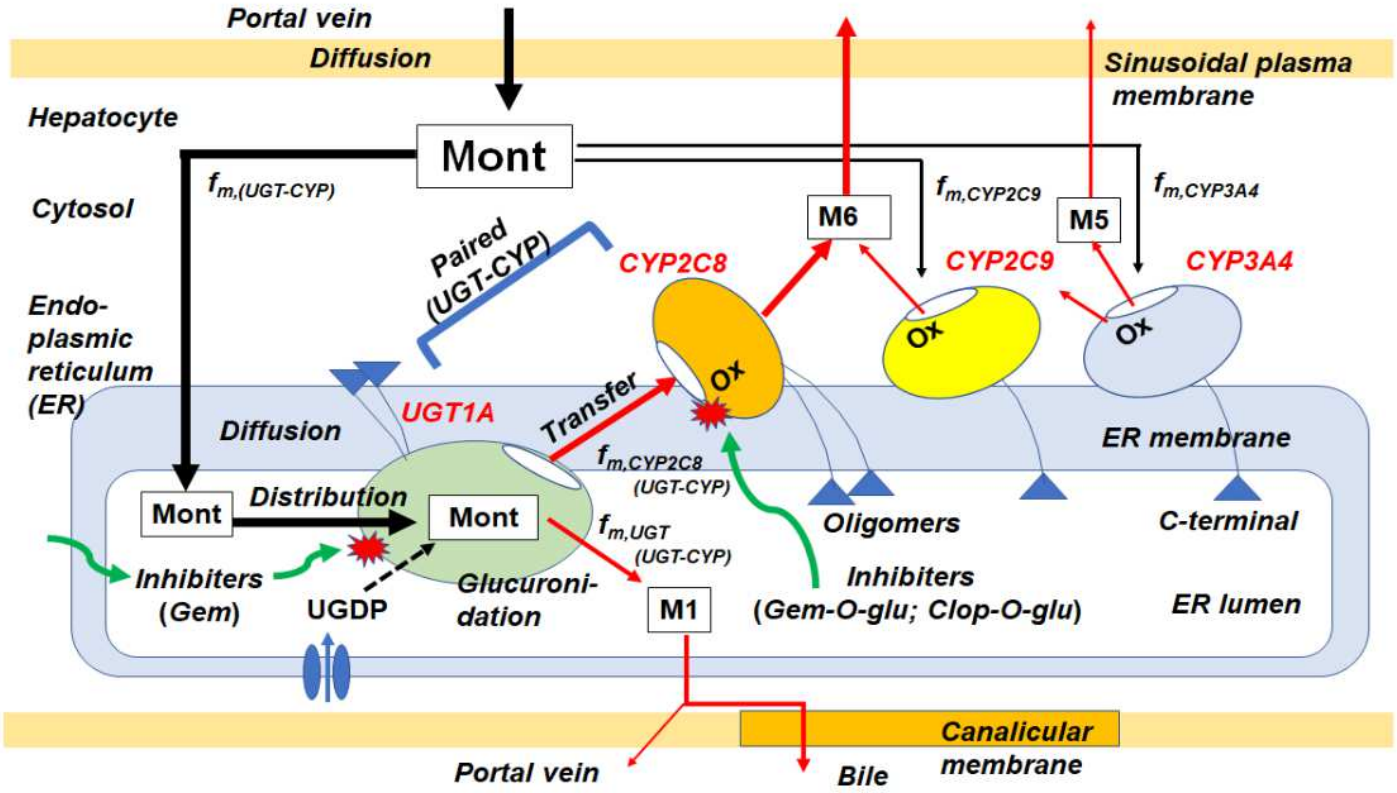

Figure 1

Illustration of a UGT-CYP paired model to analyze CYP2C8-mediated DDIs produced by Gem and Clop, with an example of Mont. The distribution of Mont into the UGT (UGT1A) from inside the endoplasmic reticulum (ER) occurs first, and then part of the drug is metabolized to M1 (acyl glucuronide) by this latent enzyme and secreted into the ER lumen as a phase II metabolite, while the remainder is transferred to the CYP2C8 that is adjacent to the UGT and thereby oxidized to a phase I metabolite. In this bi-directional metabolic pathway, Gem inhibits both UGT and CYP2C8 while Clop inhibits CYP2C8 alone. These inhibitors show increased inhibition activity against CYP2C8 after glucuronidation.

Figure 2

Illustration of how to determine the plasma metabolite levels in response to the unchanged drug levels when the first pass effect of a drug is not considered.

Figure 3

Static 2-compartment model-based simulations (SMs) of the plasma unchanged victim levels in the DDIs where Clop, Gem, or Gem + Itr victimized Mont and Des. The doses of Mont, Des, Clop, Gem and Itr were 10mg SD, 5 mg SD, 300mg then 75mg QD 3 days, 600 mg BID 3 days, and 100mg QD 3 days, respectively. (-): control; (+): coadministration; obs: observed.

Figure 4

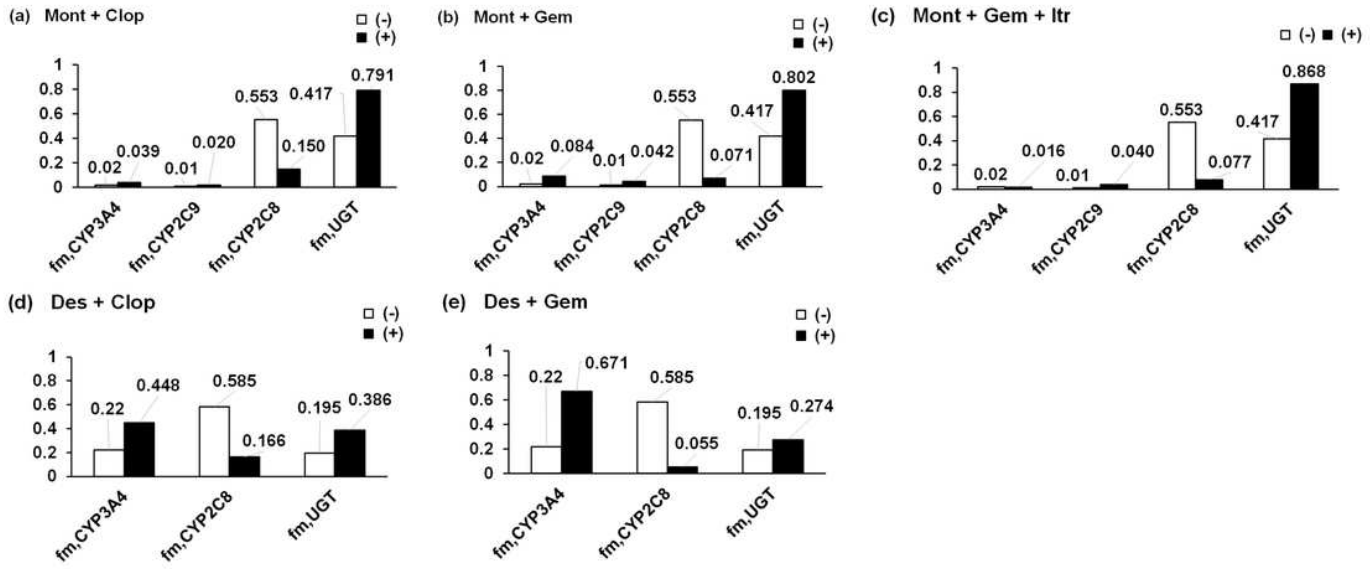

Figure 4

$f_{m,UGT}(+) = A_{i,overall}\ \ f_{m,UGT}/pA_{i,UGT(d)}$

Changes in the fractional enzymatic clearances ($f_{m,CYP}$s and $f_{m,UGT}$) determined for the Mont and Des victimized DDIs.

$f_{m,CYP3A4}(+) = A_{i,overall}\ \ f_{m,CYP3A4}/pA_{i,CYP3A4}$

$f_{m,CYP2C9}(+) = A_{i,overall}\ \ f_{m,CYP2C9}$

$f_{m,CYP2C8}(+) = A_{i,overall}\ \ f_{m,CYP2C8}/pA_{i,UGT(d)}/pA_{i,CYP2C8}$

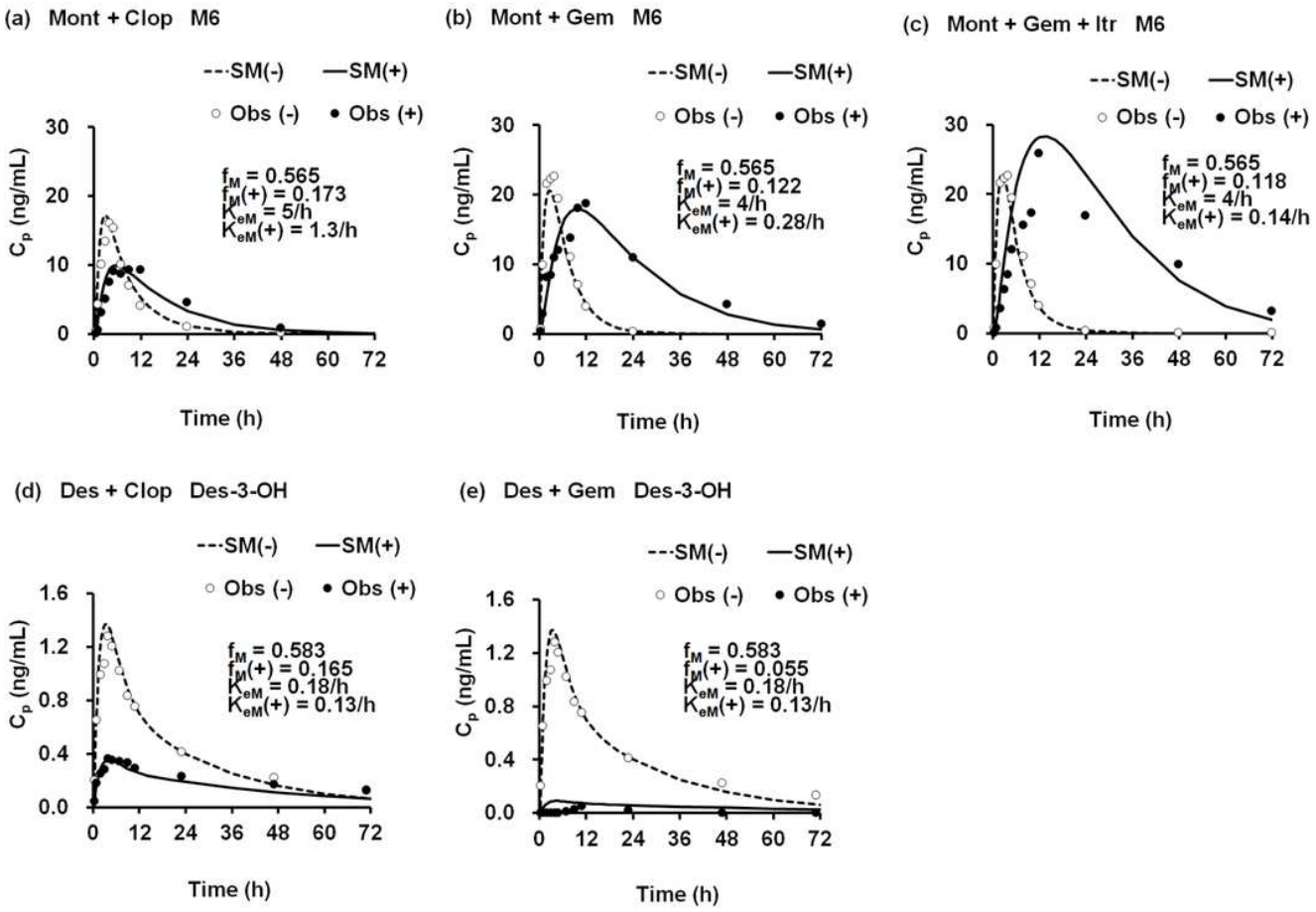

Figure 5

f_M-based SMs of the plasma levels of metabolites formed by CYP2C8, in response to the unchanged drug levels in the DDIs where Clop, Gem, or Gem + Itr victimized Mont and Des.

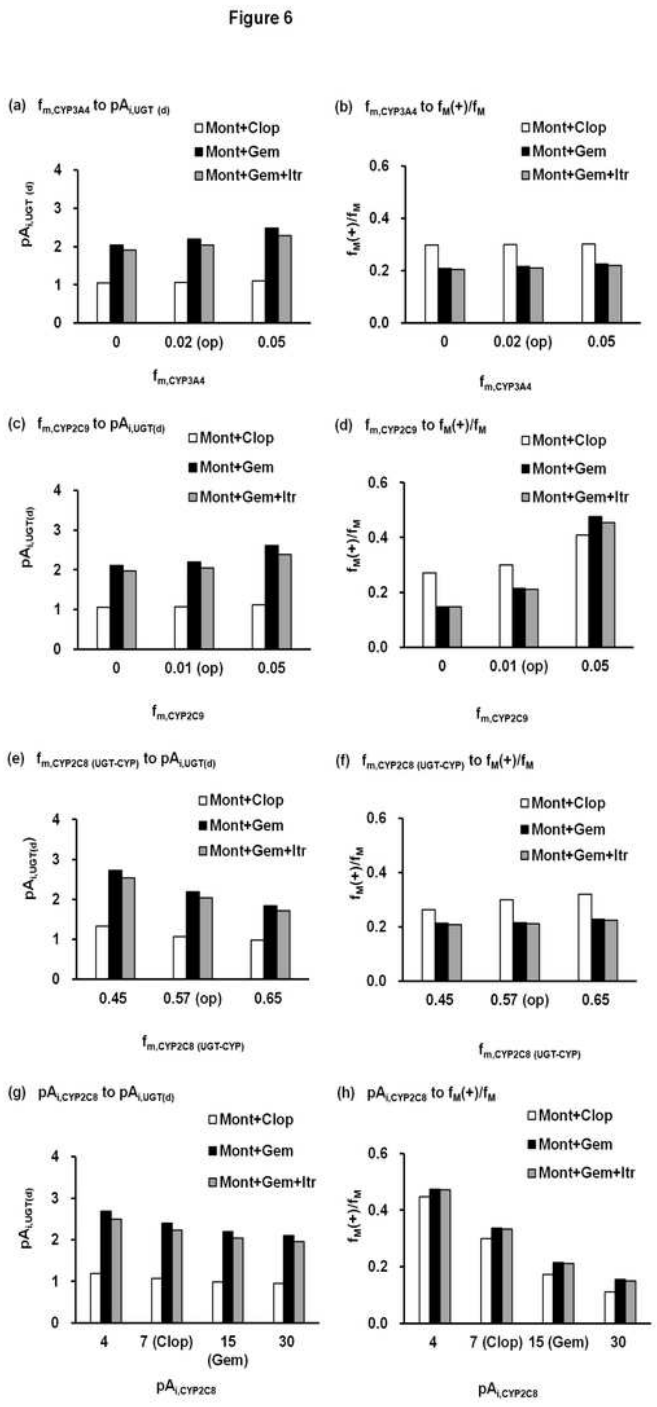

Figure 6

Sensitivity of the input parameters used in the UGT-CYP paired model analysis to $f_M(+)/f_M$ and $pA_{i,UGT(d)}$ for Mont victimized DDIs (optimal parameters are centered).

Figure 7

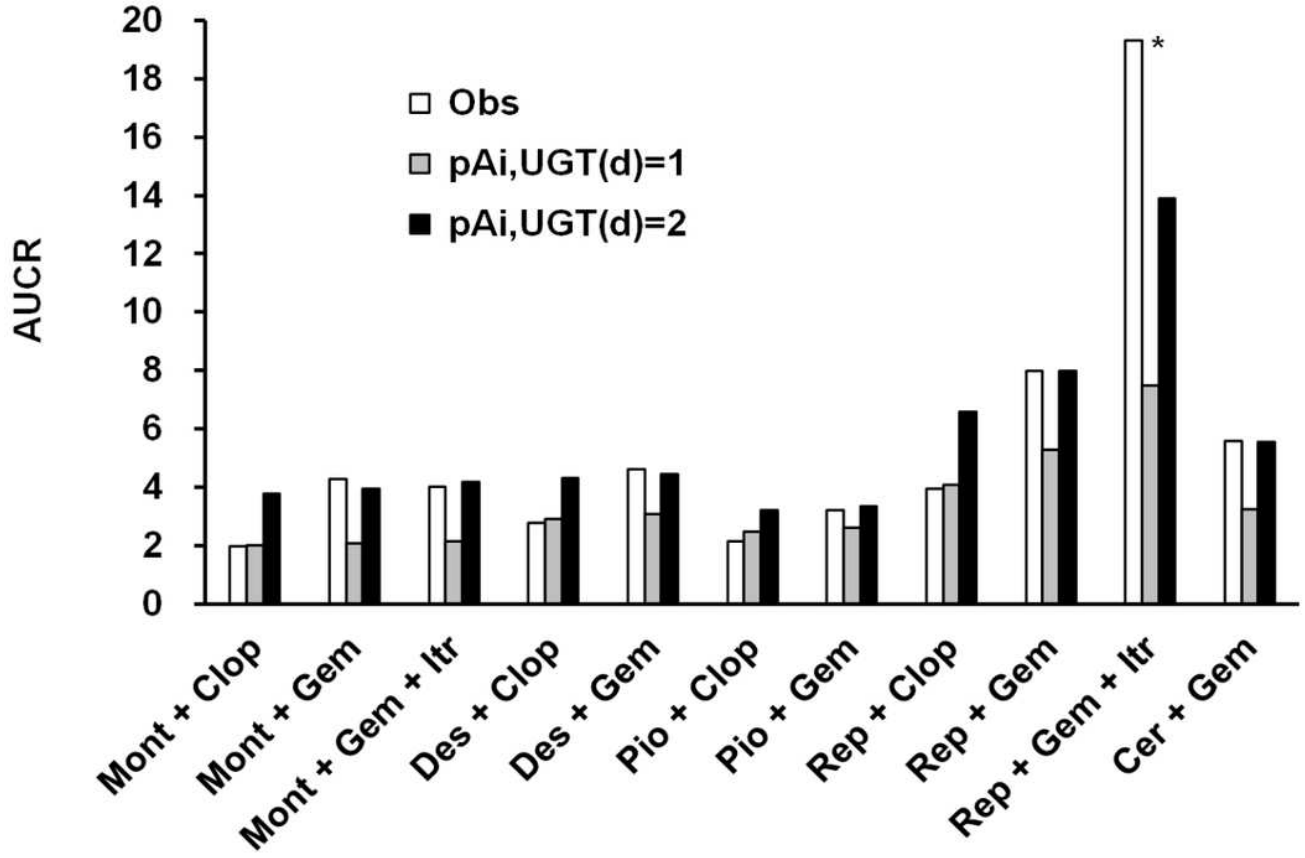

Figure 7

Prediction of AUCR for the DDIs in which Clop, Gem, or Gem + Itr victimized Mont, Des, Pio, Rep, and Cer, assuming inhibition of UGT ($pA_{i,UGT(d)}$ = 2), compared with the noninhibition ($pA_{i,UGT(d)}$ = 1). For Pio, F_h = 0.952, $f_{mCYP3A4}$ = 0.12, $f_{m,CYP2C19}$ = 0.1, $f_{m,CYP2C8}$ = 0.655 and $f_{m,UGT}$ = 0.125 were assumed. For Rep, F_h = 0.630, $f_{mCYP3A4}$ = 0.08, $f_{m,CYP2C8}$ = 0.828 and $f_{m,UGT}$ = 0.092 were assumed. For Cer, F_h = 0.844, $f_{mCYP3A4}$ = 0.10, $f_{m,CYP2C8}$ = 0.765 and $f_{m,UGT}$ = 0.135 were assumed. The observed AUCR for Rep + Gem + Itr (*) would not necessarily be accurate because the time last (7h) was too short to estimate the AUC (+) .

Supplementary Files

This is a list of supplementary files associated with this preprint. Click to download.

- CYP2C8mediatedDDISuppleM.docx